Experimental Study of Flows in a Two-Dimensional Inlet Model

Miklos Sajben,* Thomas J. Bogar†, and Joseph C. Kroutil‡
McDonnell Douglas Corporation, St. Louis, Missouri

Experimental results are reported for flows in a ramp-type, external-compression inlet with a rectangular, large-aspect-ratio cross section, at a freestream Mach number of 1.84. Variation of the exit throttle area created a wide range of operating conditions, from highly supercritical to fully subsonic internal flows with a detached shock ahead of the ramp lip. Both time-mean and dynamic aspects of the flows were investigated. At high terminal-shock Mach numbers (1.5-2.2), three different, massively separated, subsonic flow patterns were found, which depended on throttle setting and the history of prior flow conditions. A specific pressure ratio could be associated with at least two such patterns. At low pressure ratios, the terminal shock was weak and strongly influenced by the ramp/cowl configuration. The presence of leading edges is believed to have been closely involved in the large-amplitude, periodic oscillations (buzz) observed at the low end of the pressure-ratio range.

Nomenclature

A = cross-sectional area
f = frequency
h = channel height
M = Mach number
$\tilde{M}_e$ = average exit station Mach number, defined by Eq. (1)
p = pressure
R = perfect gas constant
T = absolute temperature
u = velocity
x = streamwise coordinate, $x=0$ at ramp lip, positive downstream
y = transverse coordinate, $y=0$ on flat portion of bottom wall, positive upward
z = spanwise coordinate, $z=0$ at plane of symmetry
γ = ratio of specific heats
ν_e = pressure ratio ($=p_{t\infty}/p_{se}$)
ρ = density

Subscripts

av = average
e = exit station
s = static
t = total
u = top (upper) wall
v = throttle location (vent)
σ = immediately before terminal shock
0 = at cowl lip (geometric throat)
∞ = freestream
$(\tilde{\ })$ = peak-to-peak amplitude of ensemble-averaged waveform

Superscripts

$(\tilde{\ })$ = distance normalized by h_0 (=23.5 mm), except for $\tilde{M}_e$
$(\bar{\ })$ = time = mean value
$(\hat{\ })$ = rms value of fluctuating component

Introduction

FLOWS in inlets of supersonic air-breathing propulsion systems possess several characteristic features that make their experimental investigation or theoretical prediction exceptionally difficult. The most important of these features are the shock/boundary-layer interactions (SBLI) that are always present in inlets, their detailed forms depending on the structure of the shock system of the particular inlet. The most important SBLI is associated with the terminal shock which initiates the subsonic internal flow and is invariably followed by a subsonic deceleration, sustained for a distance of many channel heights by the divergence of the channel walls. The resulting postshock adverse pressure gradient has a profound influence on the entire flow, especially if the shock Mach number is larger than approximately 1.3. Above this limit very large separated regions develop, the postshock boundary-layer thickness growth rates become extreme, and boundary layers on opposite walls merge before they recover from the effects of the interaction.[1-3] Many past SBLI studies were conducted in constant area channels or tunnels[4,5] where effects associated with a sustained postshock pressure gradient were either not present at all or were greatly suppressed. For this reason, only a few of the many published SBLI experiments are directly applicable to inlet flows.

Normal-shock/turbulent-boundary-layer interactions combined with adverse postshock gradients have been explored[1-3] using supercritically operated convergent-divergent channels (diffusers) up to shock Mach number 1.34. Diffusers properly simulate portions of inlet flowfields, including the SBLI region and the subsequent subsonic flow, provided that the terminal shock is entirely within the channel.

Another set of difficulties in the investigation of inlet flows arises from the conditions at the upstream end of the channel. In diffusers, supersonic flow is initiated at an internal geometric throat, while inlets establish a channel flow by swallowing part of a supersonic approach stream using appropriately shaped leading edges around the channel perimeter (cowl, ramp). The upstream boundary conditions created by this ingestion are fundamentally different from those in diffusers, and their consequences are not well understood, especially if the terminal shock is located sufficiently close to, or ahead of, the leading edges.

Presented as Paper 83-0176 at the AIAA 21st Aerospace Sciences Meeting, Reno, Nev., Jan. 10-13, 1983; received June 16, 1983; revision received May 3, 1984.

*McDonnell Douglas Fellow, McDonnell Douglas Research Laboratories. Associate Fellow AIAA.

†Scientist, McDonnell Douglas Research Laboratories. Senior Member AIAA.

‡Unit Chief, McDonnell Douglas Research Laboratories. Member AIAA.

The leading-edge shock system, the terminal SBLI, the decelerating subsonic flow, and the associated rapidly growing boundary layers combine to form typical inlet flows. These features interact both in time-mean and dynamic senses, giving rise to collective behavior characteristic of the combination as a whole. Furthermore, these collective phenomena tend to be of technological interest, such as the common, large-scale, self-excited inlet flow fluctuations, that may reach intolerably large amplitudes at off-design conditions and become major performance-limiting factors.[6] In ramjets, inlet fluctuations may couple with combustion instabilities and develop into large-amplitude pressure oscillations that cause engine unstart and mission failure.[7]

The objective of this paper is to explore the overall behavior of a nominally two-dimensional laboratory inlet model that incorporates the above characteristic features. The work is an extension of our previous studies into two new directions: 1) the incorporation of inlet-like initial conditions using a ramp/cowl configuration in a $M_\infty = 1.84$ supersonic freestream, and 2) the employment of terminal-shock Mach numbers up to approximately 2.2, well above the previous maximum of 1.34. Mean shock positions range from deep within the inlet (highly supercritical) to a detached position ahead of the model. Both time-mean characteristics and naturally occurring fluctuations are investigated.

The emphasis on collective behavior places severe limitations on the depth to which any particular portion of the flow can be explored. These limits are accepted as inevitable tradeoffs in return for obtaining information needed to define meaningful future studies of inlet flows.

Test Facility

Model

The inlet model (Fig. 1) is an external-compression, ramp-type inlet operated in a semi-freejet mode in the exhaust of a supersonic nozzle. The ramp angle is 14.7 deg, which in conjunction with the freestream Mach number of 1.84 produces an attached weak oblique shock, yielding a ramp-surface Mach number of 1.3. This Mach number is close to that found in typical ramjet inlets, although it may also be produced by a combination of higher freestream Mach numbers and higher ramp angles. The oblique ramp shock is designed to clear the cowl lip by 0.7 mm, so that the cowl lip is also exposed to the postshock Mach number of 1.3.

The tangent of the inside cowl surface at the lip is parallel to the flat ramp surface, and the cross-sectional area increases monotonically beyond this point so that a geometric throat ($dh/dx = 0$) is formed at the cowl lip. The height of the channel at this location ($h_0 = 23.5$ mm) is used as a reference length throughout the paper. The channel continues to diverge (maximum angle of 6.9 deg) and forms a gradual transition to a constant-area segment. The contours are simple combinations of straight lines and circular arcs; no attempt was made to optimize any performance indicator by tailoring the wall shapes.

An arbitrarily chosen location within the constant-area segment is designated as the exit station ($\tilde{x}_e = 22.1$), which corresponds to the fuel-injector location in ramjets and to the compressor face in turbojets. The exit-to-throat height ratio (h_e/h_0) is 2.68.

The channel is terminated by a device to throttle the choked cross-sectional area by symmetrically positioning hinged end segments of the wall (doors). Figure 1 also shows three additional components located between the two doors and used in a separate study of the dynamic response of the inlet to periodic downstream perturbations.[8] These components were held stationary in the present experiments, and their presence had no effect on the results presented here.

The inlet is located in the core of the supersonic flow produced by a two-dimensional supersonic nozzle. The top and bottom nozzle-wall boundary layers are removed through large slots above and below the ramp and cowl lips, respectively. Approximately 68% of the nozzle flow enters the inlet.

The nozzle and inlet form a single structural unit with common side walls that permit glass windows to overlap the gap between the nozzle and the inlet. This design ensures excellent optical access to a region where important dynamic processes occur. However, the associated lack of side-wall boundary-layer control limits the extent to which two-dimensionality can be achieved, and a large throat aspect-ratio (7.56:1) was chosen to minimize side-wall boundary-layer influence.

The nozzle is supplied with dry, filtered air from a 51-cm-diam, 160-cm-long plenum chamber immediately upstream. The plenum has several flow-control screens and a smoothly contoured transition to the nozzle with a contraction ratio of 22.4:1, providing highly uniform flow. Plenum chamber pressures ranged up to 600 kPa with mass flow rates through the nozzle of 6.7 kg/s.

Instrumentation

Fifteen channels of steady data were routinely recorded, including operational variables such as pressures in the plenum chamber and at various locations along the top wall of the nozzle and inlet model, temperatures, and rms values of selected surface pressures.

The top and bottom walls of the model contain more than 100 orifices for measuring the time-mean wall static-pressure distribution. Ten ports along the top wall and two along the bottom wall accommodate sensors for fluctuating surface pressures. Two similar ports, one each in the cowl and ramp slots, were used to detect passage of the terminal shock over the cowl and ramp lips. Miniature strain-gage-type transducers with flat frequency response to 90 kHz were used to measure the unsteady pressures. Surveys of the unsteady wall pressures were amplified, low-pass filtered at 10 kHz, and recorded on FM tape.

A vertical rake of 12 total-pressure tubes (0.8 mm o.d.) was used to measure the time-mean total-pressure distribution at the exit plane of the model. The rake could be traversed spanwise to within 1 cm of the side walls. Another vertical rake containing four fast-response pressure transducers (1.6 mm o.d.) was used to measure the time-dependent total pressures at midspan. This rake could be stepped in the vertical direction to three fixed locations, providing a 12-point resolution of the vertical variation of unsteady pressures.

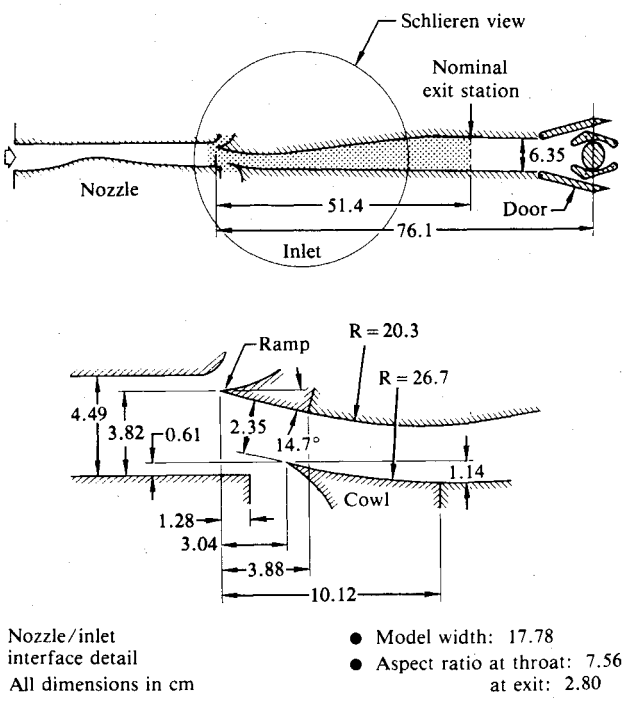

Fig. 1 Inlet model dimensions. Shaded area illustrates region of interest.

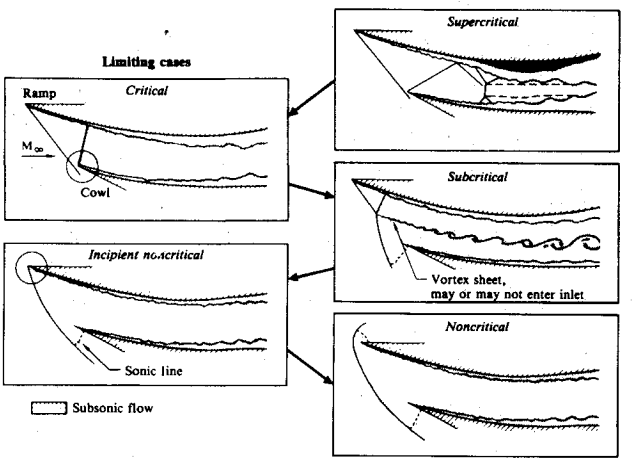

Fig. 2 States of criticality for instantaneous flows in external compression inlets. Arrows indicate decreasing throttle area.

Oil-flow traces and high-speed (5000 frame/s) and spark schlieren photography were used to visualize the flow.

Flow States

The procedure for operating the model was to open the doors fully and to pressurize the plenum sufficiently (at least 520 kPa) to cause the initially formed shock system to be swallowed by the inlet. The doors were subsequently adjusted for the desired operating condition. The terminal shock moved upstream as the doors were closed; it could be located anywhere within the inlet or driven completely into the nozzle by reducing the throttle area sufficiently.

The streamwise position of the terminal shock is used to characterize the instantaneous flow patterns, as illustrated in Fig. 2. The instantaneous flow state is termed supercritical if the terminal shock is downstream of the geometric throat, subcritical if it is between the throat and the ramp lip, and noncritical if it is ahead of the ramp lip (i.e., if the shock is detached). Singular states occur if the shock is exactly at the throat (critical) or exactly at the ramp lip (incipient noncritical).

All flows in which the shock is upstream of the throat are traditionally labeled subcritical. Designating part of this range noncritical simplifies the description of distinct flow features that occur only when the terminal shock is detached.

Having defined the various types of criticality for instantaneous flow states, it is possible to refine the existing definitions of criticality for time-mean flows. Since the streamwise position of the shock is always unsteady, the definition of time-mean criticality must be based on a finite range of shock positions, as opposed to a single distinct shock location. Since the shock motion is generally random, the range of shock positions must be specified in statistical terms, using the probability density distribution for shock position. A conceptually precise definition might be to define the range as four standard deviations centered around the time-mean shock position. If so defined, the shock would be inside this range 94% of the time.

Having determined the shock range by some method,§ the time-mean criticality can be defined. One might consider the time-mean shock position as a basis for the definition of time-mean criticality; however, most important qualitative changes of behavior were found to correlate with the upstream-most shock position. For this reason, the time-mean criticality of a given flow is defined here to be the same as the instantaneous criticality associated with the flow when the shock is located at the upstream end of the shock position range.

Instantaneous and time-mean criticalities are not necessarily the same at all instants, and failure to differentiate may result in confusion. For instance, a flow that is subcritical in the time-mean sense may temporarily assume subcritical, critical, and supercritical instantaneous states at the shock oscillates, and time-mean noncritical flows may display all five types of instantaneous criticality.

Test Parameters

The terminal shock position is the fundamental property upon which the present classification of flow conditions is based, but it is impractical for engineering use as a descriptive parameter to characterize the time-mean flow. Conventional parameter choices are the mass flow (normalized by the maximum mass flow), the overall pressure ratio (either exit-total/inlet-total or inlet-total/exit-static), and the normalized throttle area (A_v/A_0). None of these choices is completely satisfactory for the following reasons.

The normalized throttle area was under direct experimental control, and all other parameters varied as a function of door setting. However, the throttle was spatially separate from the region of interest (Fig. 1), and its setting did not explicitly indicate the conditions prevailing at the exit station, whereas knowledge of downstream boundary conditions is necessary to relate the results to theoretical considerations. Furthermore, because of the short distance between the exit station and the throttle, the flow entering the throttle was not fully developed; A_v/A_0 could not be calibrated against inlet mass flow. Therefore, the connection between this parameter and quantities of fundamental interest was specific to the test hardware and was used only in describing observations directly related to operational procedures.

The normalized mass flow is not appropriate since it is constant and therefore ambiguous over the entire supercritical range.

The pressure ratio $\nu_e(=p_{t\infty}/p_{se})$ is precisely measurable, temporally constant despite flow oscillations, and can be displayed in real time for setting the desired flow condition. The disadvantage is that ν_e reaches a minimum near critical conditions, such that values slightly greater than critical may correspond to either super- or subcritical conditions. In those near-critical ranges where such nonuniqueness of ν_e proved troublesome, the time-mean exit Mach number was adopted as the flow condition descriptor. The nonuniformity of the exit-station flow necessitated using an average, whose definition is arbitrary. A conceptually convenient averaging is given by

$$M^2_{e,\,\mathrm{av}} = \left[\int \bar{\rho}(\bar{u})^3 \mathrm{d}A \Big/ \gamma R \int \bar{\rho}\bar{u}\bar{T}\mathrm{d}A\right]_{x=x_e} \tag{1}$$

This definition stems from the integral energy equation written for a control volume enclosed by the model and bounded by a plane surface at the exit station. The surface integral associated with the exit flow contains two terms, representing the kinetic and thermal energy fluxes. $M_{e,\mathrm{av}}$, as defined by Eq. (1), is proportional to the ratio of these two terms. A practical advantage of using $M_{e,\mathrm{av}}$ is that, unlike the other parameters mentioned above, it meaningfully characterizes the entrance flow conditions for the combustor or compressor following the inlet.

Determination of the area integrals of Eq. (1) was impractical, and $M_{e,\mathrm{av}}$ was approximated by an analogous average ($\tilde{M}_e$) computed from the flow distributions at midspan only:

$$(\tilde{M}_e)^2 = \left[\int_0^{h_e} \bar{\rho}(\bar{u})^3 \mathrm{d}y \Big/ \gamma R \int_0^{h_e} \bar{\rho}\bar{u}\bar{T}\mathrm{d}y\right]_{\substack{x=x_e \\ z=0}} \tag{2}$$

§Probability densities for shock position were not determined in this study. However, shock position ranges could be determined with reasonable confidence by observing high-speed films and moving temporary end-markers on the screen until they bracketed the shock most of the time.

The integrands were determined from the known total (plenum) temperature, the the time-mean total-pressure data from a fixed, 12-tube rake located at midspan and the time-mean wall static pressure obtained as the average of pressures at four orifices located at the same streamwise station.

One-dimensional gasdynamic relations predict that the exit-station Mach number varies monotonically with A_v/A_0. This relation was also true for the experimentally determined $\tilde{M}_e$ values up to approximately $\tilde{M}_e = 0.34$ ($\nu_e = 1.3$), thereby providing the desired nonunique characterization in this range.

The presence of the side-wall boundary layers caused $\tilde{M}_e$ to be greater than $M_{e,\mathrm{av}}$. The deviation degrades the accuracy of $\tilde{M}_e$ as a measure of kinetic/thermal energy flux ratios but does not impair its utility as a unique characterization of the flow condition for $\tilde{M}_e < 0.34$. For $\tilde{M}_e > 0.34$, the flows may display significant spanwise asymmetry, which destroys the monotonic connection between $\tilde{M}_e$ and A_v/A_0 and severely increases the discrepancy between $\tilde{M}_e$ and $M_{e,\mathrm{av}}$. For this reason, only ν_e was used for flows with $\tilde{M}_e > 0.34$ ($\nu_e = 1.3$). Figure 3 illustrates the connection between $\tilde{M}_e$ and ν_e.

Boundary-Layer Patterns

Variation of the throttle area from its maximum to its minimum created a variation of $\tilde{M}_e$ from 1.07 to 0.14. Combining information from high-speed schlieren films, spark photographs, oil-flow patterns, and exit-station rake data, it was established that four qualitatively different boundary-layer patterns may occur, as illustrated in Fig. 4 and described below.

Bottom-Wall Separation

This pattern is established at the start and is characterized by a massive separation bubble on the flat bottom wall. The Mach number immediately before the terminal shock on the top wall (M_{ou}) is calculated from estimated total pressures and measured wall static pressures to be 1.72 to 2.17.¶

The supersonic flow is terminated by two oblique shocks, one on each wall, situated at approximately the same streamwise location and both inducing separation at the shock foot. The top-wall boundary layer reattaches within several boundary-layer thicknesses, while the bottom bubble grows rapidly for several channel heights in the streamwise direction, thickening to almost half of the local channel height. The flow may be supersonic over a significant central portion of the exit cross section (crosshatched shading in Fig. 4a), suggesting that the boundary-layer displacement surfaces create a convergent-divergent effective channel that causes reacceleration to supersonic speeds. The initial supersonic part of the flowfield is closely two-dimensional, but the flow beyond the terminal shock probably contains secondary flows in the form of a pair of two streamwise, counterrotating vortices, whose presence is suggested by dual peaks in the Mach-number contours at the exit station (Fig. 4a) and by oil flows.

Top-Wall Separation

The characteristics are the same as those for bottom-wall separation, except for the reversed role of the two walls at $1.53 < M_{ou} < 2.1$. Minor lateral asymmetry was observed (Fig. 4b).

Side-Wall Separation

This pattern is characterized by a lateral maldistribution of the flow, evident from oil-flow traces and Mach-number distributions at the exit station (Fig. 4c). Spark schlieren photographs are misleading in this case; they suggest comparable, moderate separation on both walls and do not indicate the asymmetry.

¶Total pressure was estimated by taking into account total pressure loss across the first oblique shock only; therefore the estimated Mach numbers are upper limits.

Exploration of spanwise flow distributions at the nozzle entrance revealed no measurable asymmetry, nor were there any measurable geometrical asymmetries in the model. The flow is sensitive to minute deviations from symmetry in geometrical configuration, initial conditions, or possibly in downstream boundary conditions.

Two-Dimensional Flow

At low terminal-shock strengths ($M_{ou} < 1.6$, $\nu_e < 1.35$), the flow was symmetric and reasonably two-dimensional over much of the span. The flow was not drastically affected by the presence of boundary layers, which were either attached or displayed only thin separated regions at the exit station (Fig. 4d).

The first three patterns were invariably supercritical, while two-dimensional flow can be associated with all three types of criticality. The patterns, however, cannot be associated with fixed time-mean parameter ranges because their occurrence depended significantly on the history of the flow.

History Effects

Two distinct sequences of viscous patterns occurred as the throttle area was varied between its extreme values. One sequence was associated with the initial pass through the exit-area range from maximum to minimum, and the other was observed throughout all subsequent manipulation of the doors, whether increasing or decreasing A_v/A_0. These two sequences are illustrated in Fig. 5.

The initial sequence started with bottom separation (Fig. 5, point A). As the doors were closed, the shock gradually moved upstream until $\nu_e = 1.8$ and $\tilde{x}_{ou} \cong 5.6$, where an abrupt transition to side separation occurred (B1→B2). Further door closing led to one of two possible paths: either a gradual forward motion of the terminal shock without a change of pattern character until point D2 or, more probably, a gradual change from B2 to C1, followed by an abrupt transition at $\nu_e = 1.7$ to a top-separated mode ($C_1 \rightarrow C2$) and an equally abrupt return to side separation at $\nu_e = 1.5$ (D1→D2). The specific sequence was selected by the flow with no apparent connection to externally controllable factors.

Subsequent door closing caused a gradual reduction of the side-wall separation bubble until a two-dimensional flow was gradually established near $\nu_e \cong 1.35$ (point E). The flow remained two-dimensional for all further exit-area reduction.

The critical condition was associated with a minimum of the pressure ratio. In the subcritical region, the pressure ratio in-

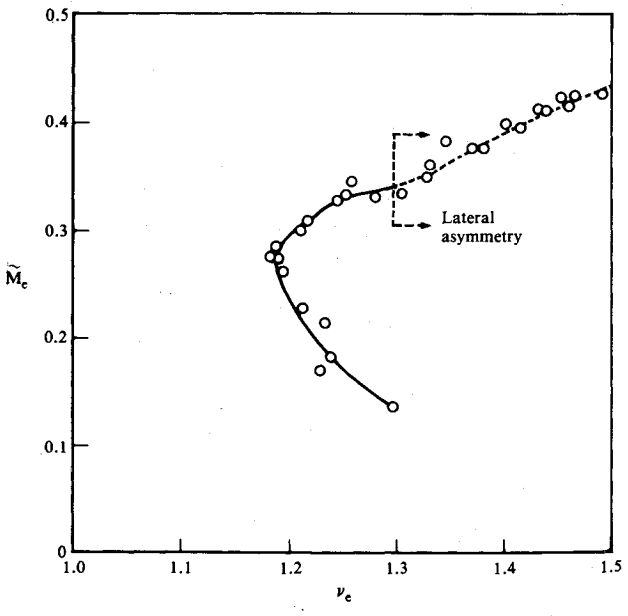

Fig. 3 Connection between test parameters ν_e and $\tilde{M}_e$.

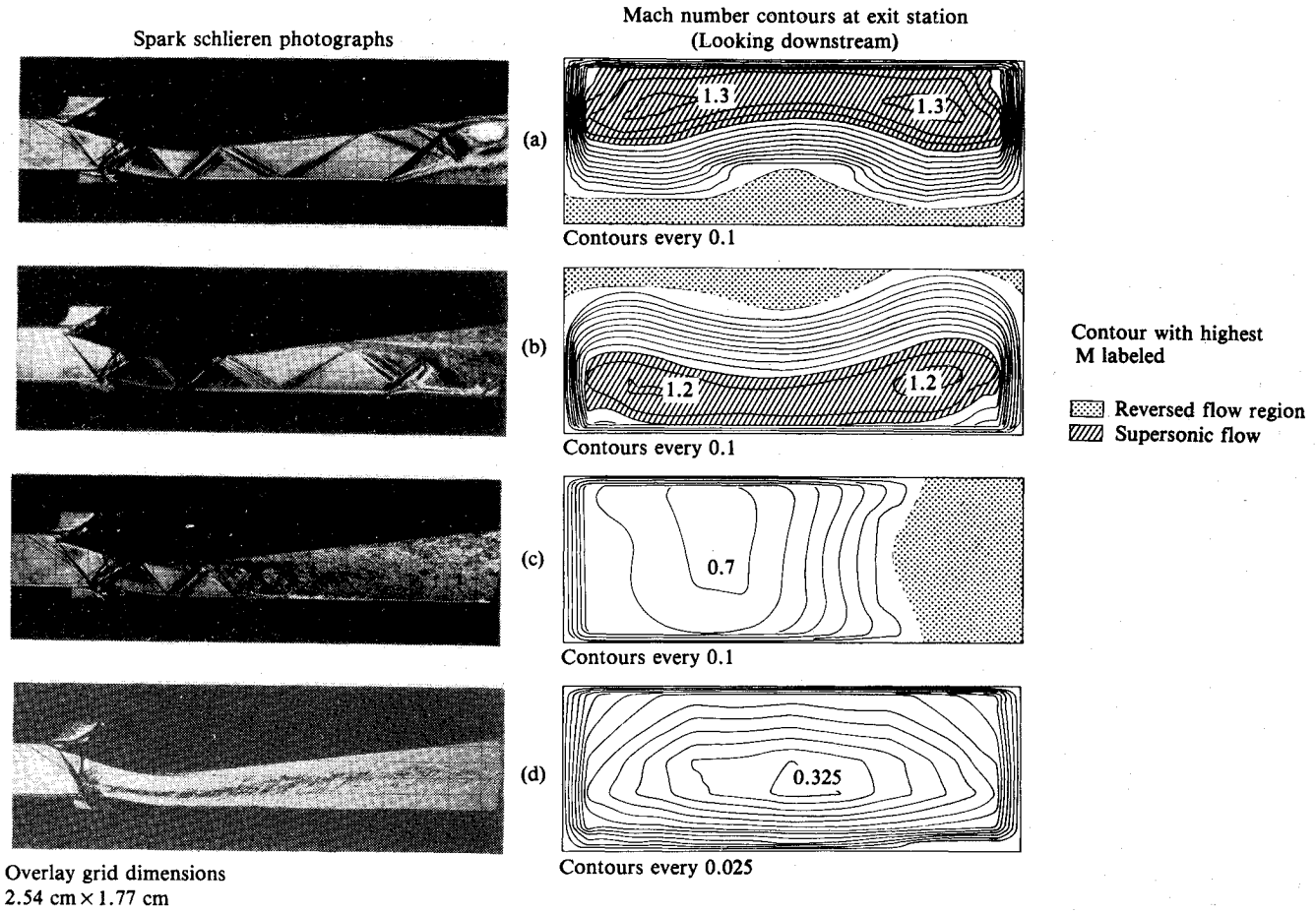

Fig. 4 Typical flow patterns: a) bottom-wall separation ($\nu_e = 3.55$); b) top-wall separation ($\nu_e = 3.55$); c) side-wall separation ($\nu_e = 1.87$); and d) two-dimensional flow ($\nu_e = 1.19$). Exit station located approximately 16 cm downstream of the field of view of the photographs (see Fig. 1).

creased as the doors were closed until the incipient noncritical condition (point F) was reached. A small, further throttle-area reduction beyond point F was sufficient to drive the shock past the incipient noncritical point without appreciably changing the pressure ratio, but large-amplitude oscillations were initiated. Additional throttling moved the terminal shock abruptly into the nozzle exit (G1→G2), where it became stationary.

As the doors were subsequently opened, the flow retraced the progression from G2 to D2, where an abrupt transition occurred into the top-separated pattern (D2→D1). The flow then remained top-separated for all greater pressure ratios, up to point H. Subsequent door manipulations, regardless of history, resulted in flow characterized by the sequence H, D1↔D2, E, F, G1.

Abrupt flow transitions were always connected with a discontinuous change in ν_e and always occurred between two massively separated patterns; transition into or out of two-dimensional flow was gradual.

History effects further aggravate the already complex problem of characterizing the operational conditions of the inlet. As indicated in Fig. 5, both A_v/A_0 and ν_e may be nonunique over certain ranges. A_v/A_0 may be nonunique either because of differences between the startup sequence and subsequent cycles or because of the erratic behavior found between points C1 and D2. ν_e may be nonunique for the same two reasons and also because of the abrupt transitions between massively separated patterns.

Two-Dimensional Flows

The remainder of this paper will be confined to the discussion of flows between points E and G1 in Fig. 5. In this range, the flow is acceptably two-dimensional, there are no history effects, and $\tilde{M}_e$ uniquely defines the time-mean condition of the flow.

Time-Mean Behavior

The top- and bottom-wall static-pressure distributions are displayed in Fig. 6. In supercritical cases ($\tilde{M}_e > 0.28$), the abrupt slope change immediately downstream of the shock in bottom-wall pressure distributions suggests a shock-induced separation (c.f., discussion and Fig. 9 in Ref. 1). This observation is in apparent conflict with the absence of separation marks from oil-flow traces taken under the same condition. Shock oscillations could conceivably prevent the development of reversed flow traces, especially if the oscillation range is greater than the length of the separation bubble. Separation is not suggested by the bottom-wall pressure distributions for supercritical conditions, or for the top wall under any condition.

These findings conflict with earlier observations[1-5] that shock-induced separation occurs at terminal-shock strengths $M_0 \gtrsim 1.3$. In the present experiment, top-wall shock Mach numbers ranged up to 1.6 (for $M_e \leq 0.42$), yet the top-wall boundary layers appear to be attached. On the other hand, bottom-wall-shock Mach numbers stayed below 1.29 (for $\tilde{M}_e \leq 0.42$), yet separation is strongly suggested by the surface pressure distributions. No explanation is available at present for this discrepancy.

Time-Dependent Behavior

The inlet flows displayed some unsteadiness at all operating conditions; the terminal shock was never stationary. The intensity and spectral content of the fluctuations depend on the

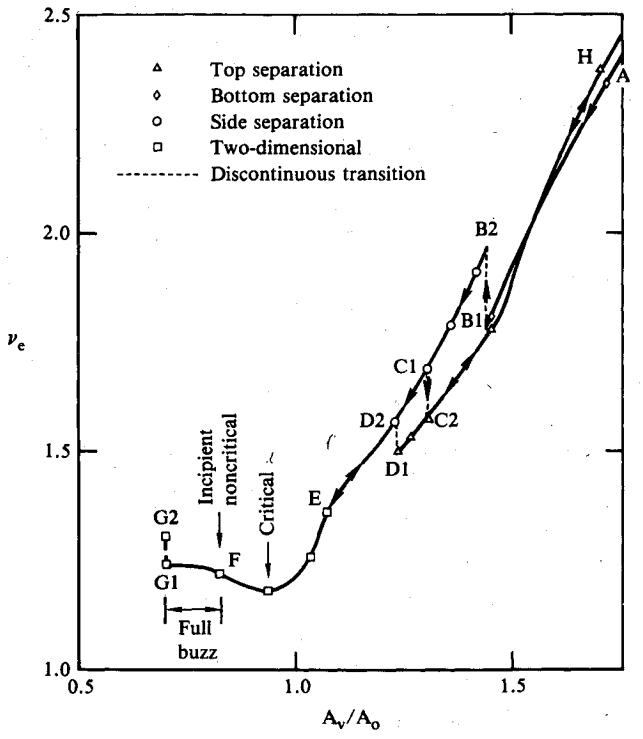

Fig. 5 Nonuniqueness and history effects.

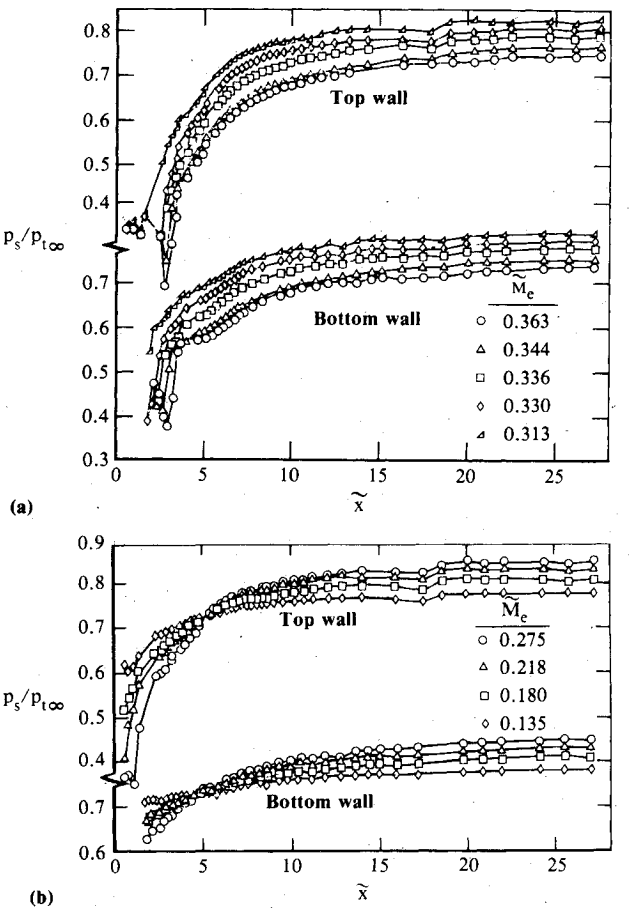

Fig. 6 Wall-pressure distributions: a) supercritical; b) critical and subcritical.

mean operating condition of the inlet. Figure 7 illustrates the observed shock-position ranges as a function of $\tilde{M}_e$. Ranges of time-mean criticality (in terms of $\tilde{M}_e$) are also indicated.

The fluctuations can be classified conveniently on the basis of the associated shock-position ranges. If the shock position fluctuates without changing the instantaneous criticality of the flow, the respective motions are termed purely supercritical, subcritical, or noncritical** oscillatory modes.

If the shock-position ranges overlaps two adjacent criticality states, then the oscillations are designated as dual modes. Depending on the criticalities involved, two types of dual modes can occur; they are distinguished by the qualifiers super/sub or sub/non.

Finally, the shock-position range may extend over all three ranges of criticality; the oscillation is then called a triple mode. As shown in Fig. 7, triple mode observed in the present experiments was characterized by extremely large amplitudes; the flow displayed all patterns on Fig. 2 in periodic succession.

The term "buzz" has been used in the literature to describe various types of fluctuations. Traditional usage appears to be best preserved if buzz is defined to include all oscillations in which periodic changes of instantaneous criticality occur, i.e., the dual and triple modes. Buzz will thus be viewed as a broad category, to be subdivided as necessary to characterize various versions.

The overall fluctuation levels vary with the mean-flow conditions according to Fig. 8, which illustrates the wall pressure-fluctuation (rms) intensity at the exit station and at $\tilde{x}=4.23$ on the ramp surface. The latter is close to, and always downstream of, the terminal shock in the $\tilde{M}_e$ range shown. This figure shows that the fluctuation intensity is smallest at the critical condition and that streamwise variation of the amplitudes over the subsonic region is small.

Figure 9 illustrates the total-pressure fluctuation intensity (rms) profiles at the exit station for two conditions. The distribution for the supercritical case indicates two peaks, presumably representing an incomplete merger of the top- and bottom-wall boundary layers. Since the shock/boundary-layer interaction does not cause separation on either wall, the boundary-layer growth rate is moderate, and merging is still in progress at the exit station.

The fluctuation profile measured during triple-mode buzz is uniform, which is compatible with photographic evidence showing that the boundary layers are too thin to be resolved by the 12 interior points used here. The local Mach numbers are low, and the measured fluctuations result primarily from static pressure variations, in contrast to the supercritical case where velocity fluctuations supply the dominant contributions.

Figure 10 traces development of the power spectral density distribution (PSD) determined from top-wall pressure fluctuations measured at the exit station as the flow condition varied from supercritical to triple-mode buzz. For supercritical flows near criticality (Fig. 10a), the fluctuations are near minimum intensity (Fig. 9), with nearly constant contributions over a broad frequency band up to 10 kHz and no particularly significant spectral structure. The absence of identifiable peaks was unexpected since earlier studies of supercritical diffuser flows[2] displayed systematic sets of well-defined peaks. No explanation was found for the absence of peaks.

If $\tilde{M}_e$ is reduced slightly below its critical value (0.28), a distinct spectral peak appears at approximately 80 Hz, while the broadband motion remains a major contributor (Fig. 10b). This spectrum appears to be typical for a dual-mode oscillation.

Figure 10c illustrates that the PSD in triple mode is dominated by periodic contributions. The large number of significant higher harmonics indicates that the wave shape is distinctly nonsinusoidal.[9]

The character of wall-pressure spectra is thus related to the mode of oscillation. This relation may prove to be helpful in identifying the oscillation mode in developmental situations

**In the present semi-freejet arrangement purely noncritical, oscillations were not observed. In inlets exposed to an unconfined freestream, noncritical oscillations are kinematically possible.

where pressures may constitute the only dynamic information available.

Purely Subcritical Oscillation ($0.22 < M_e < 0.26$)

Under subcritical conditions, the terminal shock did not cause a visible boundary-layer separation or other observable changes in the top-wall boundary-layer, and the bottom-wall boundary layer remained subsonic throughout this range. Therefore, the shock/boundary-layer interaction did not have a dominant influence on the mean or fluctuating flowfield.

The principal feature of the flows was the vortex sheet initiated at the bifurcation point of the initial oblique and terminal shocks. The vortex sheet entered the inlet at all subcritical conditions.

The discontinuity across the vortex sheet can be characterized by the ratio of mass flows or densities on the two sides. This ratio is defined by the freestream Mach number and the ramp angle and can be calculated using the oblique shock relations, specifying the flow directions and static pressures to be the same on both sides of the sheet.[9] For the present experiment, the calculated mass flow ratio is 0.770 and the density ratio is 0.955, representing considerable initial shear.

The vortex sheet is unstable and develops into a turbulent free shear layer, growing rapidly in the adverse-pressure-gradient environment of the diverging channel (Fig. 4d) and eventually merging with the two-wall boundary layers near the end of the divergent section. The turbulence intensities at and after the mergers are high, mixing is rapid, and total-pressure profiles at the exit station show no residual signs of the velocity discontinuity.

As the time-mean shock position gradually moves from cowl lip to ramp limp, total-pressure losses increase because an increasingly large fraction of the entering fluid has higher entropy, having passed through a single, nearly normal shock instead of the two oblique shocks adjacent to the ramp.

Dual Mode (Super/Sub, $0.26 < \tilde{M}_e < 0.28$)

In this mode the terminal shock moved in and out of the inlet, bracketing the cowl lip. The displacements were moderate, and the shock generally stayed within one throat height of the cowl lip. The motion had a significant periodic contribution, with a narrow spectral peak at 64 Hz on a top-wall pressure PSD.

Triple Mode ($\tilde{M}_e < 0.22$)

Oscillation in this mode involved passage of the terminal shock through all states illustrated in Fig. 2, from noncriticality to significant supercriticality, followed by the reverse of the sequence. The motion was rigorously periodic; the periodic oscillation dominated any random, turbulence-related contributions. The shock-displacement amplitudes were far greater than in any of the other modes (Fig. 7), and pressure-fluctuation amplitudes increased rapidly as $\tilde{M}_e$ was decreased (Fig. 8).

Schlieren movies indicate a moderate, pressure-gradient-induced separation on the top wall during that small portion of the cycle when the shock is supercritical and moving upstream. For the rest of the cycle, no significant separation is visible, and the oscillation does not appear to be dependent on boundary-layer effects or shock/boundary-layer interactions. The free shear layer within the inlet is the most striking visual feature. As the shock moves through the subcritical range from cowl lip to ramp lip, the shear layer traverses the flow in the upward direction, while a downward traverse occurs when the shock is moving downstream. Triple buzz is thus associated with inherently two-dimensional features, at least during the subcritical portions of the cycle.

The streamwise distributions of top-wall pressure oscillation amplitudes are shown in Fig. 11. Ensemble-averaged pressure wave shapes were obtained at all locations shown, indicating that the fluctuations are nearly in phase throughout the inlet, such that the oscillation approximates a standing wave. The fluctuation intensity profile at the exit station (Fig. 9) shows little vertical variation; the vortex-sheet-related transverse variations have decayed completely.

Comments

Strong terminal shocks ($M_o \gtrsim 1.5$) introduced several phenomena not observed in earlier studies. The most important of these is the existence of more than one possible flowfield for a given pressure ratio: up to three were found. All three patterns were obtained by purely supercritical manipulations of the shock position, implying that identical supersonic flows preceded each flow pattern. The downstream end of the flow was a contraction section followed by a choked throat, which was unlikely to vary to any significant degree. Since the in- and outflow boundary conditions were essentially the same for all three patterns, they are believed to represent a true nonuniqueness, and not the consequences of some unintended variation of the boundary conditions.

It is reasonable to believe that the left-wall separation shown in Fig. 4c is the result of a minor, undetected initial

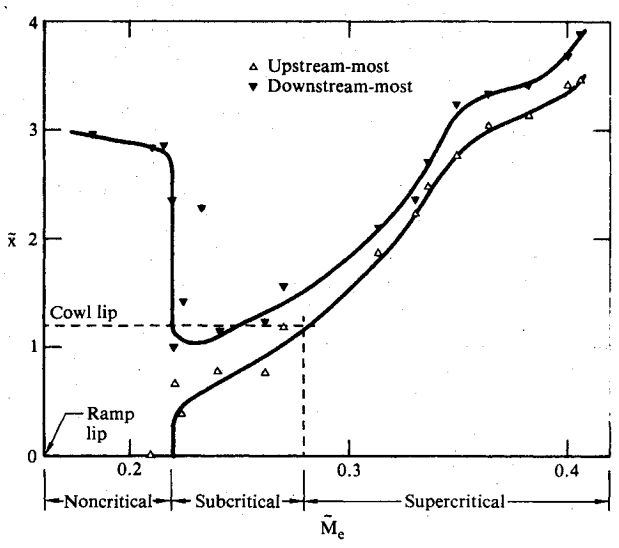

Fig. 7 Ranges of shock-position extremes and ranges of criticality for time-mean flow conditions.

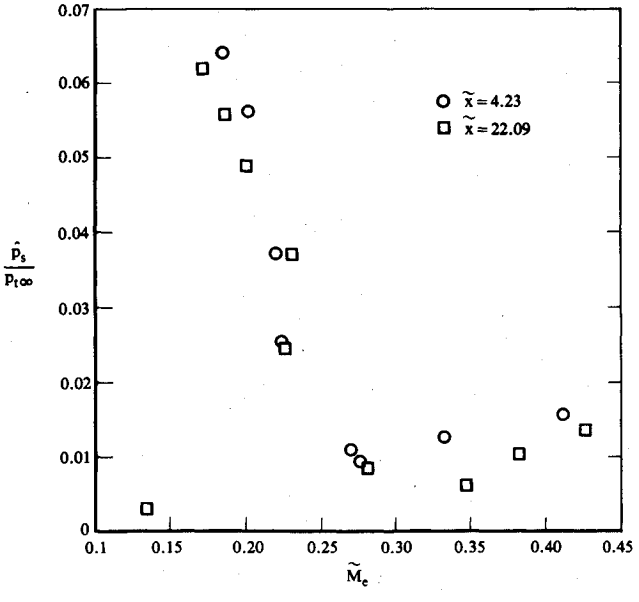

Fig. 8 Top-wall static-pressure fluctuation intensity (rms) at two streamwise locations.

asymmetry that was permanently present at all flow conditions but became important only for a certain pressure ratio range.

Nonuniqueness in supersonic flows is not new; the starting problems of supersonic tunnels and mixed-compression inlets are textbook examples. The nonuniqueness observed in this work differs from these classic cases in that the three observed flows were equivalent in terms of a one-dimensional description; they differed from each other in two- or three-dimensional aspects.

Transition between two massively separated patterns was always abrupt. Presumably each pattern had a distinct range of throttle settings under which it could exist and be stable to small disturbances. When the throttling process reached the end of the permissible range for the prevailing pattern, a transition had to occur to another pattern that was allowable at the new throttle setting.

The challenge of predicting flows that contain strong terminal SBLIs thus includes the determination of not just one but all possible patterns. Furthermore, reliability of the prediction demands some assurance that all possible solutions have indeed been found.

Details of the nonunique behavior and the dependence on throttle-setting history are specific to the configuration investigated here, but similar phenomena could certainly occur in other developmental inlet models. The detection of different flow patterns at one fixed throttle setting may be difficult because the differences may have little influence on overall parameters, such as mass flow or pressure recovery. There may be, however, large differences in flow distributions at a given cross section, which may have serious consequences on the performance of fuel-injector assemblies, combustors, or compressors.

The consequences of initiating the channel flow by swallowing part of a freestream appear to be minor in the context of time-mean flows. The boundary layers entering the terminal-shock interaction may be laminar and thinner than is usually the case in comparable diffuser tests, in which the test article must accept the test-facility boundary layer with a long past history. This difference in boundary-layer properties is probably related to the unusually high-shock Mach number associated with incipient separation on the ramp surface (1.7 instead of the expected 1.3).

In contrast, the cowl-and-ramp configuration appears to have a major effect on inlet dynamics and may even be directly responsible for the introduction of an instability that leads to the spectacularly high-amplitude triple-mode oscillations. Several factors suggest that this oscillation is driven by a basically inviscid mechanism: the precise periodicity of the motion, the absence of higher (turbulence) frequencies from the shock motion, the well-behaved core flow and the quite thin boundary layers all suggest that the dominant wave mechanism sustaining the triple mode is acoustic. Convective disturbances, which dominate the supercritical oscillations, are negligible in this case. Similar conclusions were reached by Stoolman[10] in an experimental study of normal-shock inlets.

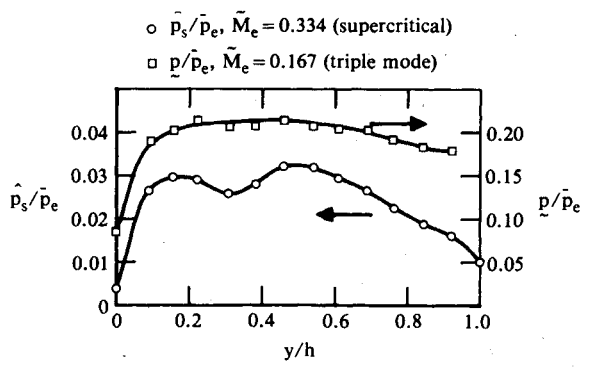

Fig. 9 Unsteady total-pressure profiles at exit station.

The triple mode is a unique acoustic oscillation, distinguished by an upstream boundary condition that changes discontinuously every time the shock passes over the cowl or the ramp lip. When the shock is inside the channel, the subsonic flow is bounded by the terminal shock, which is known to reflect acoustic waves arriving from downstream only weakly.[11] When the shock is outside, then the flow within the channel and around the lips is subsonic, with some of the approach flow spilling around the lips. It is not clear how acoustic waves are reflected from such a flow configuration, but there are reasons to believe that the reflection is stronger than that coming from a normal shock.[10] Such a switch in the nature of the boundary conditions occurs twice at the cowl and twice at the ramp in each cycle. The occurrence of the switch depends on the shock location, which is a dependent variable, such that the process is nonlinear.

Ferri and Nucci[12] proposed that buzz occurs when the vortex sheet formed at the bifurcation point of the ramp shock and terminal shock enters the inlet. (They used the term buzz to describe what is called the triple mode in this paper.) In the present experiment, vortex-sheet ingestion always occurred during buzz, but ingestion did not necessarily lead to the onset of buzz. The onset of vortex-sheet ingestion generally coincides with the passage of the shock over the cowl lip, i.e., with a discontinuous change in the boundary conditions. It is suggested that the latter may be the more important of these two nearly simultaneous events.

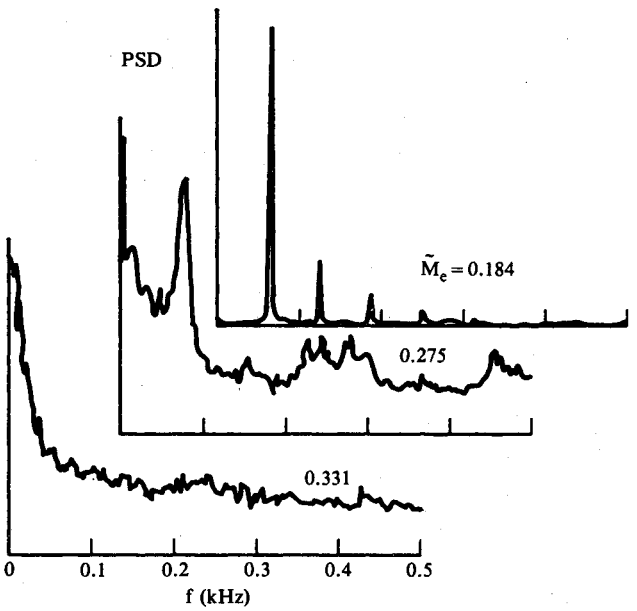

Fig. 10 Top-wall pressure PSD distributions; $\tilde{x} = 22.09$. Vertical scales are arbitrary, all scales linear.

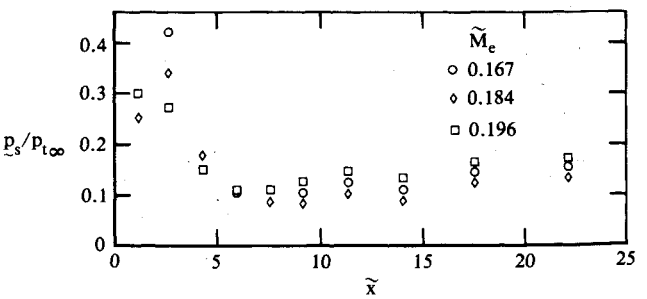

Fig. 11 Peak-to-peak amplitude of fluctuating top-wall pressures during triple mode buzz (fundamental harmonic only).

Summary

Detailed experiments were conducted in an external-compression, ramp-type inlet model with a large-aspect-ratio, rectangular cross section, using a semi-freejet test configuration with a freestream Mach number of 1.84 at zero incidence. The inlet was tested over an extreme range of operational conditions, from highly supercritical to fully subsonic internal flow, with a detached shock ahead of the inlet.

At supercritical conditions, the flows displayed strong terminal SBLIs with shock Mach numbers up to 2.2. The strong interactions led to three qualitatively different subsonic flow patterns, each characterized by the location of a massive flow separation: on the top, bottom, or side wall. Two or three separated patterns could occur at one throttle setting, depending on the history of prior flow conditions. Transitions from one pattern to another occurred abruptly as the throttle setting was changed gradually. Initial boundary conditions were the same for all strong-shock patterns.

At low pressure ratios, the SBLIs were weak and of little consequence. The flows were dominated by the largely inviscid effects associated with the proximity of the terminal shock to the leading edges (ramp, cowl) of the inlet. Under subcritical conditions the vortex sheet initiated by the bifurcation of the initial oblique and terminal shocks developed into a turbulent free shear layer that broadened to nearly half the duct height at the end of the divergent channel section.

Spontaneous fluctuations, observed at all operating conditions, were classified according to the ranges of shock positions assumed during the motion. Supercritical oscillations are dominated by the SBLIs and display broadband spectral character, while oscillations involving sub- and noncritical states appeared to be driven by inviscid mechanisms, producing significant periodic spectral contributions in dual modes and a rigorously periodic, intense oscillation in the triple mode.

Acknowledgments

The authors appreciate valuable comments and advice from Mr. M. H. Heinz of the McDonnell Douglas Astronautics Company, Mr. P. H. Hall of the Naval Weapons Center, and Mr. T. Rogers and Mr. A. E. Heins of the Marquardt Company. The authors are also indebted to Mr. H. R. Welge and Mr. R. W. Parker of the Douglas Aircraft Company for the design of the supersonic nozzle contours. This work was sponsored by the McDonnell Douglas Corporation Independent Research and Development program.

References

[1]Sajben, M. and Kroutil, J. C., "Effects of Initial Boundary-Layer Thickness on Transonic Diffuser Flows," *AIAA Journal,* Vol. 19, Nov. 1981, pp. 1386-1393.

[2]Bogar, T. J., Sajben, M., and Kroutil, J. C., "Characteristic Frequency and Length Scales in Transonic Diffuser Flow Oscillations," AIAA Paper 81-1291, 1981.

[3]Salmon, J. T., Bogar, T. J., and Sajben, M., "Laser Velocimeter Measurements in Unsteady, Separated, Transonic Diffuser Flows," AIAA Paper 81-1197, 1981.

[4]Kooi, J. W., "Influence of Free-Stream Mach Number on Transonic Shock-Wave Boundary-Layer Interaction," National Aerospace Laboratory NLR, Amsterdam, Rept. NLR MP 78013U, May 1978.

[5]Delery, J. M., "Investigation of Strong Shock Turbulent Boundary Layer Interaction in 2-D Transonic Flows with Emphasis on Turbulence Phenomena," AIAA Paper 81-1245, 1981.

[6]"Propulsion System Flow Stability Program (Dynamic)," AFAPL-TR-68-142, 1968.

[7]Rogers, T., "Ramjet Inlet/Combustor Pulsations Study," NWC TP 6209, Dec. 1980.

[8]Sajben, M., Bogar, T. J., and Kroutil, J. C., "Dynamic Response of Ramjet Inlets to Downstream Perturbations," Office of Naval Research, Final Report, MDC Q0784, Jan. 1983; also AIAA Paper 83-2017, 1983.

[9]Sajben, M., Bogar, T. J., and Kroutil, J. C., "Experimental Study of Flows in a Two-Dimensional Inlet Model," AIAA Paper 83-0176, 1983.

[10]Stoolman, L., "Investigation of an Instability Phenomena Occurring in Supersonic Diffusors," Ph.D. Thesis, California Institute of Technology, Pasadena, 1953.

[11]Culick, F. E. C. and Rogers, T., "The Response of Normal Shocks in Diffusers," *AIAA Journal,* Vol. 21, Oct. 1983, pp. 1382-1390.

[12]Ferri, A. and Nucci, L. M., "The Origin of Aerodynamic Instability of Supersonic Inlets at Supercritical Conditions," NACA RM L50K30, Jan. 1951.